ORIGINAL RESEARCH

Intravenously-injected gold nanoparticles (AuNPs) access intracerebral F98 rat gliomas better than AuNPs infused directly into the tumor site by convection enhanced delivery

Henry M Smilowitz,[1]
Alexandria Meyers,[1] Khalil
Rahman,[1] Nathaniel A
Dyment,[2] Dan Sasso,[1] Crystal
Xue,[3] Douglas L Oliver,[4]
Alexander Lichtler,[5] Xiaomeng
Deng,[6] Sharif M Ridwan,[1]
Lauren J Tarmu,[7,8] Qian Wu,[9]
Andrew L Salner,[10] Ketan R
Bulsara,[11] Daniel N Slatkin,[12]
James F Hainfeld[12]

[1]Department of Cell Biology, University of
Connecticut Health Center, Farmington,
CT, [2]Department of Orthopedic Surgery,
University of Pennsylvania, Philadelphia, PA,
[3]George Washington University School of
Medicine, Washington, DC, [4]Department of
Neuroscience, University of Connecticut
Health Center, Farmington, CT,
[5]Department of Reconstructive Sciences,
University of Connecticut Health Center,
Farmington, CT, [6]David Geffen School
of Medicine at UCLA, Student Affairs
Office, Los Angeles, CA, [7]Department of
Human Behavior, College of Southern
Nevada, [8]Department of Anthropology,
University of Nevada, Las Vegas, NV,
[9]Department of Anatomic Pathology,
University of Connecticut Health Center,
Farmington, [10]The Gray Cancer Center,
Hartford Hospital, Hartford, [11]Division of
Neurosurgery, UConn Health, Farmington,
CT, [12]Nanoprobes, Inc, Yaphank, NY, USA

Correspondence: Henry M Smilowitz
Department of Cell Biology, University of
Connecticut Health Center, 263 Farmington
Avenue, Farmington, CT 06030, USA
Tel +1 860 679 2710
Fax +1 860 679 1269
Email smilowitz@uchc.edu

Background: Intravenously (IV)-injected gold nanoparticles (AuNPs) powerfully enhance the efficacy of X-ray therapy of tumors including advanced gliomas. However, pharmacokinetic issues, such as slow tissue clearance and skin discoloration, may impede clinical translation. The direct infusion of AuNPs into the tumor might be an alternative mode of delivery.

Materials and methods: Using the advanced, invasive, and difficult-to-treat F98 rat glioma model, we have studied the biodistribution of the AuNPs in the tumor and surrounding brain after either IV injection or direct intratumoral infusion by convection-enhanced delivery using light microscopy immunofluorescence and direct gold visualization.

Results: IV-injected AuNPs localize more specifically to intracerebral tumor cells, both in the main tumor mass and in the migrated tumor cells as well as the tumor edema, than do the directly infused AuNPs. Although some of the directly infused AuNPs do access the main tumor region, such access is largely restricted.

Conclusion: These data suggest that IV-injected AuNPs are likely to have a greater therapeutic benefit when combined with radiation therapy than after the direct infusion of AuNPs.

Keywords: gold nanoparticles, glioma, edema, IV injection, convection-enhanced delivery, fluorescence microscopy, gold enhance

Introduction

Every year >22,000 people in the USA are diagnosed with primary brain tumors, with 13,000 deaths; the 5-year survival rate is 24%. For glioblastoma (GBM) multiforme, <10% of patients survive for >3 years.[1] Primary brain tumors also account for 20% of cancers in children. More effective treatments of malignant brain tumors are desperately needed.

Urgent neurosurgery is typically performed to remove the primary brain tumor and relieve dangerous intracranial pressure. However, recurrence of brain tumors is generally inevitable. The problem is that at the time of diagnosis, tumor cells have already migrated as much as 4 cm from the main tumor mass.[2–4] Unfortunately, the migrated tumor cells cannot be removed by surgery and effective radiotherapy cannot be applied over such a large volume. Further chemotherapy agents are largely ineffective in preventing recurrence. Here, we propose that gold nanoparticles (AuNPs) are targeted to migrating tumor cells, thereby selectively enhancing radiotherapy.

Hainfeld et al[5–8] pioneered the use of AuNPs to enhance the radiotherapy of tumors. In previous work, we showed that nanogold-enhanced radiosurgery of a very aggressive orthotopic glioma in mice resulted in 50% long-term survival (>1 year) compared to 0% with radiosurgery alone.[8] In those studies, the AuNPs were intravenously (IV) administered and accumulated preferentially in the tumors; ratios of gold in tumor to normal brain were ~19:1. To load tumors with enough gold to obtain these extraordinary dose enhancements (~400%), large quantities of AuNPs need to be injected. While the AuNPs used have shown no signs of toxicity to date, the injection of such large quantities of AuNPs presents a number of pharmacokinetic challenges including poor whole-body clearance, cost, and cosmetic issues (long-term skin discoloration). The direct introduction of AuNPs into the tumor region would solve many of these issues. The goal of this study is to compare the distribution of IV-injected AuNPs with AuNPs infused intratumorally by convection-enhanced delivery (CED).

A number of studies have shown that escaping tumor cells migrate into the peritumor edema, often along blood vessels (BVs) and white matter tracts.[9,10] In this study, we investigated the hypothesis that AuNPs could travel in the peritumor edema after they are infused into the primary tumor site and reach disseminated tumor cells. The AuNPs, because of their smaller size, might "catch up" to and surround migrating tumor cells. If the gold distribution was specific to the tumor, gold concentrations might be administered that would lead to significantly enhanced radiotherapy. A radiotherapy dose enhancement factor of ~4 (boosting 25 to 100 Gy) has been calculated to be possible if the gold concentration was 2% by weight.[11] Thus, the normal brain would be spared, since the electrons ejected from the gold only travel a short distance and tightly confine the boosted radiation dose.[12] Moreover, this approach would cause radiation-resistant cancer stem cells as well as dormant and drug-resistant tumor cells to be killed, since the targets of the ejected electrons and the free radicals produced are the DNA of the tumor cells and other sensitive cell machinery, rather than any particular metabolic pathway. This approach overcomes previous concerns, including the cost of an IV injection of gold, the loading of other organs and tissues, and whole-body clearance, as a much smaller amount of gold is needed locally; the gold will no longer have to pass through a leaky endothelium – it is administered directly to the edematous space in which the tumor cells reside.

F98 rat glioma cells first described by Kobayashi et al[13] were transduced with mCherry red fluorescent protein, and tumors were orthotopically grown in brains of isogeneic rats. IV-injected AuNPs were compared with AuNPs directly infused into F98 gliomas growing in the rat brain by CED. CED[14–16] is a very slow injection via a pump that better allows the injectate to travel in the interstitial space or edema than a more rapid injection. The small AuNPs were visualized in the light microscope after gold enhancement, and the coincidence of AuNPs and tumor cells was studied histologically. Edema was visualized with fluorescein isothiocyanate (FITC)-labeled anti-albumin.[17]

The results show that IV-injected AuNPs localize more specifically to intracerebral tumor cells and to the tumor edema than do the directly infused AuNPs; this is likely due to the ability of IV-injected AuNPs to better target tumor cells through a disrupted endothelial barrier, whereas directly infused AuNPs appear to have less-specific localization to the tumor cells due to disrupted generalized diffusion possibly due to encountering diffusion barrier material in the interstitial space around tumor cells.

Materials and methods

All the work and study protocols performed were approved by the University of Connecticut Health Center's Animal Care and Use Committee and adhered to the rules set forth in the Guide for the Care and Use of Laboratory Animals.

F98 cell line

The F98 cell line was purchased from the American Type Culture Collection (ATCC; Manassas, VA, USA).

Rat anesthesia

Rat anesthesia for surgical procedures was an intramuscular (im) injection of 54 mg/kg ketamine and 5 mg/kg xylazine.

Transduction of F98 glioma cells stably expressing mCherry red (F98CR)

One milliliter of 9 L medium (Dulbecco Modified Eagle's Medium [DMEM] + 10% Penicillin/Streptomycin [Penn/Strep] + fungizone) containing 6 μM polybrene + 1/100 dilution of virus stock (10⁷/mL) was added to 80% confluent F98 cells. After ~3 h, the wells were replaced with 9 L medium. This procedure was repeated on day 2. On day 3, the confluent cells were harvested and plated at ~1 cell/well (400 wells at 100 μL/well). Wells were screened by fluorescence microscopy. Highly expressing cells were cloned and used for the experiments below.

Stereotactic implantation of F98CR intracerebrally in syngeneic rats

After a midline incision to expose the scalp, a 0.6 mm burr hole was drilled at a point ~4 mm to the left of the midline along the serrated coronal suture of anesthetized Fisher 344 rats. The rats were then mounted on a David KOPF Instruments

(KOPF) stereotactic frame and the head aligned and coordinates recorded such that the bregma and lambda sutures were in the same horizontal plane. A 27 G needle mounted vertically on the frame ($Z = 0$ when just touching both the bregma and lambda sutures) was then manually adjusted until it could be inserted into the burr hole and used to deliver 10,000 F98CR cells in 1 µL, 4.5–5 mm beneath the skull into the left striatum, over ~60 s. After an additional 30 s, the needle was removed slowly over 1 min. The wound on the top of the head was repaired with Vet Bond.

Direct stereotactic intratumoral infusion of AuNPs

Approximately 3 weeks after the implantation of 10,000 F98CR cells, the anesthetized rats were similarly positioned on the stereotactic frame using the same strategy and coordinates as described (Stereotactic implantation of F98CR intracerebrally in syngeneic rats). The AuNPs were delivered at the same depth as described (Stereotactic implantation of F98CR intracerebrally in syngeneic rats) also using a 27 G needle mounted on the stereotactic frame and attached to a BS800 syringe pump (Braintree Scientific, Braintree, MA, USA) set to deliver 10 µL of AuNPs (AuroVist 15 nm, 200 mg Au/mL; Nanoprobes, Inc, Yaphank, NY, USA) over 30 min. The needle was removed slowly over 1 min, and the skin wound was repaired with Vet Bond. AuNP infusions into the left hemisphere of control rat brains without brain tumors were performed similarly.

Femoral vein injection of AuNPs

Anesthetized Fisher 344 rats with advanced F98CR tumors were placed on a surgical board (Germfree Labs, Miami, FL, USA). A small, 3 mm incision was made in the groin region of appropriately positioned rats. A hemostat was used to tease apart soft tissue exposing the femoral vein, and ~80 mg of 15 nm AuNPs (AuroVist 15 nm) were injected IV in 0.4 mL.

Perfusion fixation of rats

Deeply anesthetized rats were perfused transcardially with normal saline followed by 4% buffered formalin pH 7.4 (Fisher Healthcare, Pittsburgh, PA, USA) 24 h after IV injection and direct intratumoral infusion of AuNps.

Rat euthanasia

The euthanasia procedure, CO_2 narcosis, is done using the Euthanex system, a method approved in the Guidelines on Euthanasia by the American Veterinary Medical Association and by the University of Connecticut Health Center's Animal Care and Use Committee.

Cryosections of rat brains

Formalin-perfused/fixed rat brains were excised and incubated in 4% buffered formalin for 4 h at 4°C. The brains were then transferred to 30% sucrose in PBS for 24 h for cryopreservation. The brains were cut coronally through the site of tumor implantation and arranged tumor-face down in cassettes containing Cryomatrix (Thermo Fisher Scientific, Waltham, MA, USA) prior to rapid freezing in 2-methylbutane cooled in dry ice. The cassettes were stored at −20°C prior to sectioning. Brain tissues were cut into 7-µm-thick sections using a Cryostat (cat #: CM 3050S; Leica Microsystems, Wetzlar, Germany) at approximately −22°C–26°C, and adhesive tape (cat #: 62800-72; CryoJane) was used to transfer the sections onto adhesive slides (cat #: 62800-X; CryoJane). Sections were cross-linked to the slides with a UV-light source (cat #: CM 3050S-3-1; Leica Microsystems). Slides were stored at 4°C overnight prior to antibody staining.

Immunofluorescence

Slides were rehydrated in PBS for 10 min at room temperature (RT) and blocked with 200 µL PowerBlock for 30 min prior to the addition of primary antibodies and then incubated overnight at 4°C in a humidified chamber. Primary antibodies used were as follows: A: sheep antirat albumin: FITC, polyclonal immunogloubin G (IgG) (1:100, cat #: 0220-2424; Bio-Rad Laboratories Inc., Hercules, CA, USA), B: rabbit anti-Iba-1 (1:500, cat #: 019-19741; Wako Pure Chemical Industries, Ltd., Osaka, Japan), C: mouse antirat TUJ1 (1:1,000, cat #: MO15013; Neuromics), D: anti-GFAP (1:500, cat #: Z0334; Dako Denmark A/S, Glostrup, Denmark), and E: goat antimouse/rat CD31 polyclonal IgG (1:100, cat #: AF3628-SP; R&D Systems, Inc., Minneapolis, MN, USA). Slides were washed 3× with PBS for 5 min each prior to the addition of secondary antibodies for 60 min at RT. Secondary antibodies used were as follows: I: goat antirabbit IgG (H + L) cross-adsorbed secondary antibody, Alexa Fluor 488 (1:500, cat #: A-11008; Thermo Fisher Scientific), and II: goat antimouse IgG (H + L) cross-adsorbed secondary antibody, Alexa Fluor 647 (1:200, cat #: A-21235; Thermo Fisher Scientific). The primary and secondary antibodies were paired as follows: A, not paired, edema; B:I, microglia; C:II, neurons; D:I, astrocytes; and E:II, endothelial cell. Finally, slides were washed 3× for 5 min each with PBS; coverslips were mounted in glycerol:PBS (1:1) containing a 1:1,000 dilution of Hoechst (DAPI) (cat #: 62249; Thermo Fisher Scientific).

Gold enhance

Gold enhance (GoldEnhance™ LM; Nanoprobes, Inc) was performed according to manufacturer's recommendations

GoldEnhance catalytically deposits additional gold on the small AuNPs so that their location can be seen in the light microscope. Background was reduced by transferring water-washed slides (~5 min) into 15% sodium sulfite solution (~5 min) and then water washed prior to cover slip mounting.

Fluorescent microscopy

Images were first taken of regions with red and green fluorescence using a Zeiss Axio Scan.Z1 microscope using the Zen 2.3 software. The slides were then gold enhanced and reimaged. The fluorescent- and gold-enhanced images were then aligned as individual layers in Photoshop, but most analyses were done on side-by-side comparisons of fluorescent- and gold-enhanced images.

Data analysis

Migration of tumor cells away from the main tumor mass

A straight line was drawn in Photoshop between the center of each migrating cell and the nearest defined edge of the tumor mass. The number of pixels in the new line was then proportionally divided by the number of pixels in the scale bar to calculate the metric migration distance.

Diameters of BVs containing tumor cells

Diameters were measured by drawing straight lines across the largest and the smallest diameters of each eligible BV. For each distinct BV, the number of pixels in each of its two diameter lines was averaged, and the average diameter was then proportionally divided by the number of pixels in the scale bar to calculate its metric diameter.

AuNP content of F98-containing BVs

F98-containing BVs were scored semiquantitatively for AuNP content after gold enhancement. The level of AuNP observed was classified as negative (−), relatively low (+), and relatively high (++).

Results

F98 rat gliomas were confirmed to be invasive: tumor cells were found far from the main tumor mass, usually in association with BVs and peritumor edema

Figure 1A shows that large numbers of tumor cells (red) were found distal to the margins of the main tumor mass, usually around structures that resembled BVs. The tumor (Figure 1A) measures ~1,100 × 600 µm. Tumor cells lining BV could be seen up to 1,100 µm away from the margins of the main tumor mass. Individual mCherry positive tumor cells could

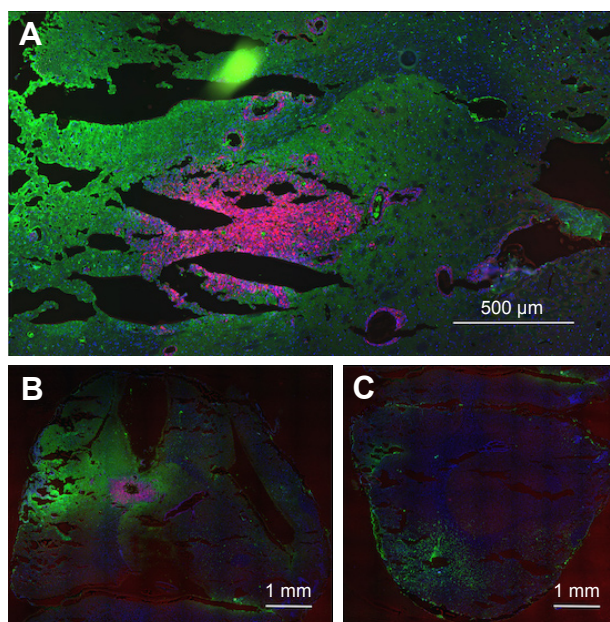**Figure 1** Tumor cells and edema in the brains of rats with advanced F98 gliomas. **Notes:** (**A** and **B**) Left hemisphere (two separate rats) and (**C**) right hemisphere. (**A–C**) mCherry red (tumor, red), anti-albumin (edema, green), and DAPI (nuclei, blue).

also be seen in these regions. In general, the tumor cells lining the BV were two to six cells thick, as determined by counting DAPI-stained nuclei. A total of 85% of the BV lined by tumor cells had areas ranging from 100 to 2,000 µm² (median 363 µm), 13.5% were larger, between 2,000 and 10,000 µm², and 1.5% were associated with structures up to 150,000 µm². Figure 1B shows that the tumor containing left hemisphere had more FITC albumin stain (edema) than the right hemisphere (Figure 1C) that is devoid of tumor cells. Bright FITC staining could be seen around the central tumor mass and the region around the tumor insertion needle track.

IV-injected AuNPs track with tumor

Figure 2A and E is the low power image of left hemispheres containing mCherry red expressing F98 tumors (two separate rats) and Figure 2B and F is the corresponding image, after gold enhancement. IV-injected AuNPs were found in the same brain areas as tumor and peritumor edema. The corresponding right hemisphere images (Figure 2C, D, G, and H) are devoid of both tumor and AuNPs. Left and right hemispheres are devoid of enhanced gold in saline-injected rats (Figure 3A–D).

IV-injected AuNPs track with tumor cells and tumor edema

Tumor cells that have migrated away from the main tumor mass are usually seen to have gold associated with them
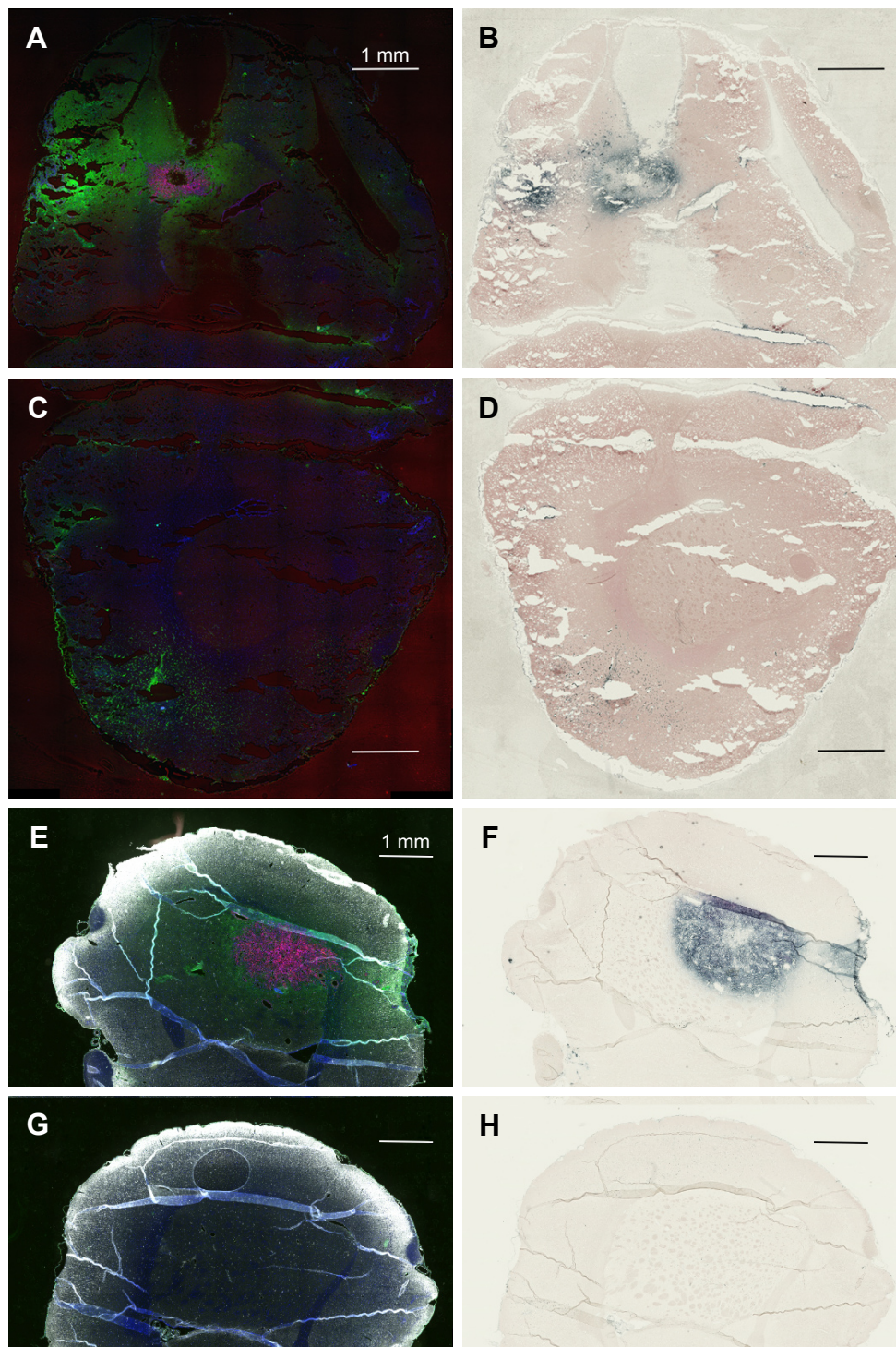
Figure 2 IV-injected AuNPs colocalize with F98 tumors. (**A**) Rat 1, left hemisphere, fluorescence; (**B**) Rat 1, left hemisphere, gold enhance; (**C**) Rat 1, right hemisphere, fluorescence; (**D**) Rat 1, right hemisphere, gold enhance; (**E**) Rat 2, left hemisphere, fluorescence; (**F**) Rat 2, left hemisphere, gold enhance; (**G**) Rat 2, right hemisphere, fluorescence; and (**H**) Rat 2, right hemisphere, gold enhance. (**A–G**) mCherry red (tumor, red), anti-albumin (edema, green), DAPI (nuclei, blue), and anti-CD31 (blood vessels, white) and (**B–F**) gold enhanced (gold stained, black).
Abbreviations: AuNPs, gold nanoparticles; CD31, cluster of differentiation 31; IV, intravenous.

after IV injection of AuNPs (Figure 4A and B). Interestingly, the gold is often seen lining the perimeter of the tumor cells creating a cobblestone-like appearance. This gold labeling is specific, as it is not seen in saline-injected controls (Figure 4C and D). Figure 4C shows tumor cells typically surrounding a BV that is clearly stained white with the endothelial marker anti-CD31. The most intense gold stain leaks out where there is edema. FITC-albumin staining (edema) is typically brightest around BVs associated with migrating tumor cells. This is shown in Figure 5A and B.
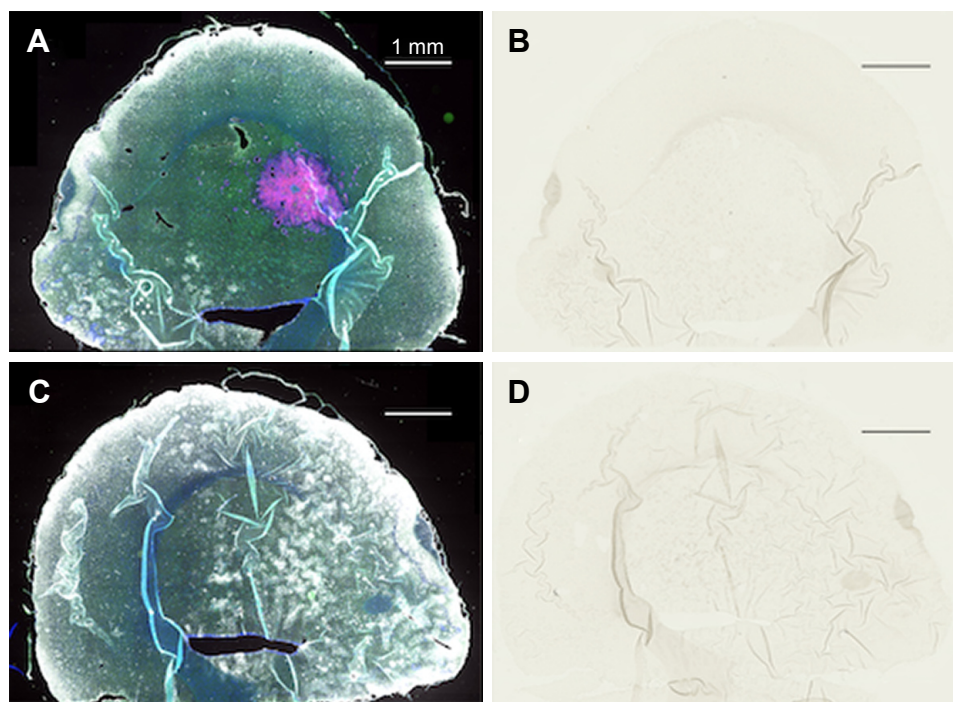
Figure 3 Complete lack of gold enhancement in saline-injected rats.
Notes: (**A**) Left hemisphere, fluorescence; (**B**) left hemisphere, gold enhance; (**C**) right hemisphere, fluorescence; and (**D**) right hemisphere, gold enhance. (**A** and **C**) mCherry red (tumor, red), anti-albumin (edema, green), DAPI (nuclei, blue), and anti-CD31 (blood vessels, white) and (**B** and **D**) gold enhanced (gold stained, black).
Abbreviation: CD31, cluster of differentiation 31.

Direct stereotactic infusion of AuNPs into the established brain tumor

Inspection of the brains revealed that much of the infused dose could be found along the corpus callosum and a white matter tract called the external capsule, which is lateral to the corpus striatum (Figure 6A and B). The corresponding right hemisphere that did not receive an AuNP infusion did not show gold labeling (Figure 6C and D). Figure 6E shows the neuronal layer as revealed by TUJ-1 staining, and the position of the major white matter tracts containing gold (drawing, 6F) beneath the neuronal layer. Some of the AuNPs were also found in the region of the brain surrounding tumor (Figure 6A and B); however, most of the AuNPs did not penetrate the main tumor mass (Figure 6B).

Figure 6B (inset control) shows the infusion of AuNPs into the left hemisphere of a rat brain without a tumor; AuNPs diffuse through the hemisphere. Figure 6D (inset control) shows the corresponding right hemisphere to the Figure 6B (inset).

Most of the directly infused gold does not reach the tumor cells that are surrounding BVs

Interestingly, there was a relative lack of AuNPs in or around the tumor cells surrounding BVs (Figure 7A–D). The data

are summarized in pie charts (Figure 8). The greatest difference between IV and directly injected AuNPs was seen in the main tumor mass, where the majority of F98 (+) BVs had AuNPs after IV injection but not after direct injection. The peritumor region also showed a higher correlation of AuNP++ with tumor-associated BVs.

AuNPs that are infused directly into rat brains are taken up by microglia and astrocytes

Figure 9 shows the uptake of AuNPs into brain microglia and astrocytes after the injection of AuNPs directly into control brains (no tumor). Microglia, identified by Iba-1 staining, and astrocytes, identified by GFAP staining, were shown to have taken up the AuNPs identified by gold enhancement. The cells taking up AuNP, as shown in Figure 9A, are identified as microglia by virtue of the Iba-1 staining, as shown in Figure 9B. The cells taking up AuNP in Figure 9C are identified as astrocytes by virtue of the GFAP staining, as shown in Figure 9D. Arrows indicate correspondence between fluorescence and gold staining. The data show that both microglia and astrocytes stain for AuNPs.

Discussion

The F98 glioma[13] is a nonimmunogenic, moderately radiation-insensitive, invasive, aggressive, and rat glioma model that
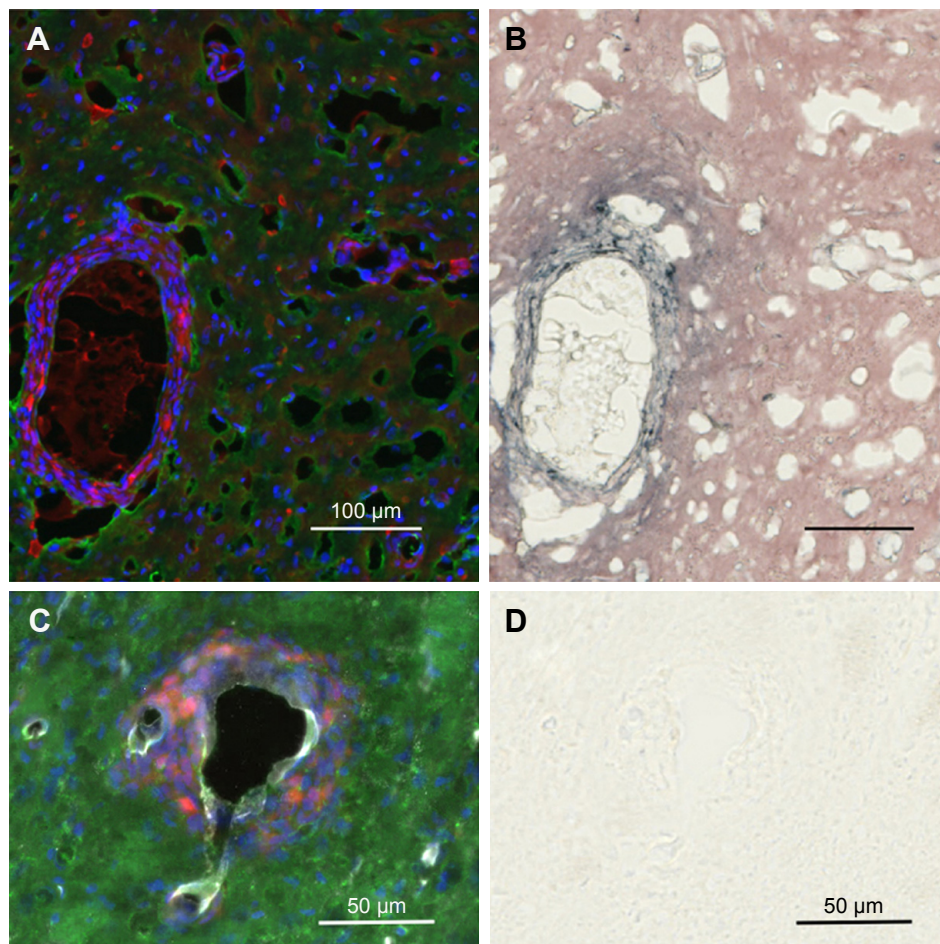
Figure 4 IV-injected AuNPs are associated with tumor cells lining blood vessels far from the main tumor mass.
Notes: Region far from the central tumor: (**A**) fluorescence and (**B**) gold enhanced. Saline control far from the central tumor: (**C**) fluorescence and (**D**) gold enhanced. (**A** and **C**) mCherry red (tumor, red), anti-albumin (edema, green), DAPI (nuclei, blue), and anti-CD31 (blood vessels, white) and (**B** and **D**) gold enhanced (gold stained, black).
Abbreviations: AuNPs, gold nanoparticles; CD31, cluster of differentiation 31; IV, intravenous.

is difficult to treat.[18] Its invasive properties are corroborated in Figure 1 in which tumor cells can be seen lining BVs at least one tumor diameter distal to the main tumor mass. This property of high-grade gliomas has been known for

Figure 5 IV-injected AuNPs are found around tumor cells lining blood vessels and edema in peritumor region.
Notes: Peritumor region: (**A**) fluorescence, mCherry red (tumor, red), anti-albumin (edema, green), DAPI (nuclei, blue), and anti-CD31 (blood vessels, white) and (**B**) gold enhanced (gold stained, black). Scale bar, 50 μm.
Abbreviations: AuNPs, gold nanoparticles; CD31, cluster of differentiation 31; IV, intravenous.

many years[19] and is reproduced by this model. It poses one of the central problems faced by the clinician when treating GBM. High-grade gliomas usually arise as unifocal lesions and are usually discovered when they are large (>3 cm in largest diameter) and occupy ~2% of the human brain. If tumor cells have already migrated one or more tumor diameters away from the main tumor mass, the volume of brain containing tumor is already too large for full surgical removal or highly effective radiation therapy. The standard of care chemotherapy using the best drug known, temozolomide, only provides 1–3 more months of life extension. Other therapies, including immunotherapy[20] and cytotoxic viral therapy,[21] may have the potential to kill these outlying tumor cells. We hypothesize that radiation therapy could contribute more to the control of the migrated cells if methods were developed, whereby therapeutic radiation doses could be precisely and selectively delivered to the outlying tumor cells.

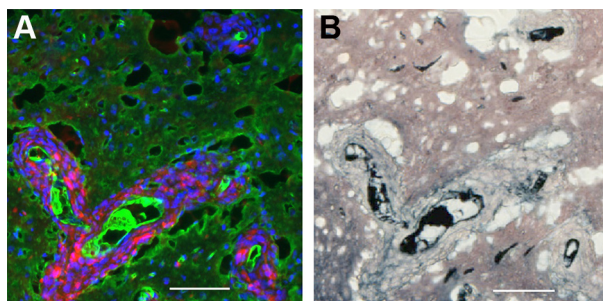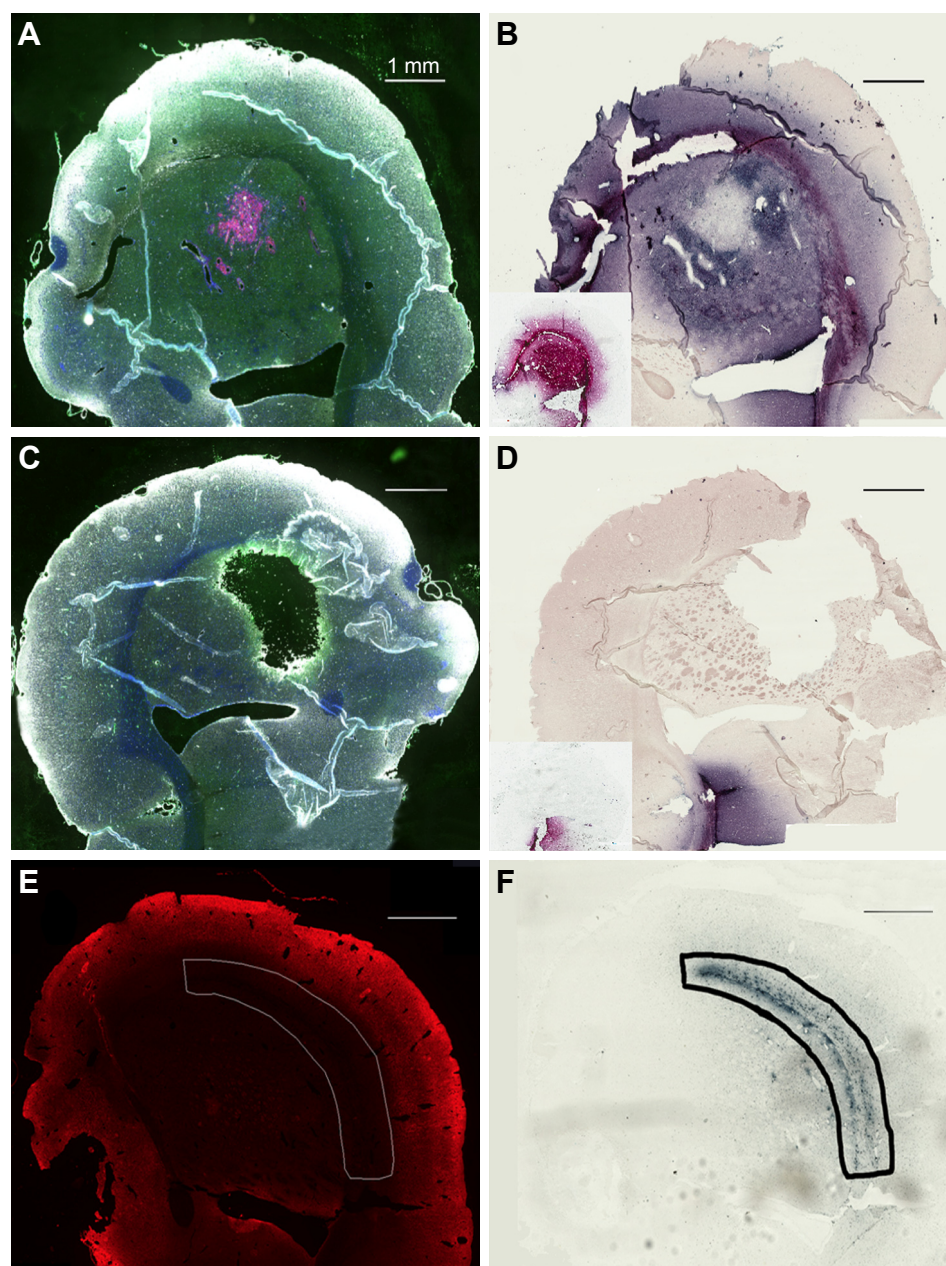AuNP-enhanced radiation therapy was first shown to effectively treat subcutaneous tumors[5] and then gliomas

Figure 6 Directly injected AuNPs are found in the white matter track and peritumor region but not in the main tumor region.
Notes: (**A**) Left hemisphere, fluorescence; (**B**) left hemisphere containing a brain tumor, gold enhanced; (**B**, inset) left hemisphere with no brain tumor, gold enhanced; (**C**) right hemisphere, fluorescence; (**D**) right hemisphere, gold enhanced; (**D**, inset) right hemisphere with no brain tumor; and (**E**) another animal, left hemisphere, stained for neurons (anti-Tuj 1, red fluorescence). (**A** and **C**) mCherry red (tumor, red), anti-albumin (edema, green), DAPI (nuclei, blue), and anti-CD31 (blood vessels, white) and (**B**, **D**, and **F**) gold enhanced (gold stained, black).
Abbreviations: AuNPs, gold nanoparticles; CD31, cluster of differentiation 31.

in mice[8] using nontoxic, well-tolerated AuNPs developed by Nanoprobes, Inc. Theoretical calculations have shown that loading tumors with AuNPs to 2% w/w increases the radiation dose to the tumor by about fourfold.[11] Hainfeld et al[8] showed that loading advanced gliomas in mice to such levels is feasible due to the leakiness of vessels within these tumors.[22,23] Achieving such high AuNP levels in tumors requires injecting a very large amount of AuNPs by the

IV route. The AuNPs are designed to circulate for a long time ($t_{1/2} = \sim24$ h) to maximize leakage into the tumor but ultimately most of the AuNPs are taken up by macrophages, predominantly in the liver and spleen.[8] Although AuNP doses >4 g/kg are well tolerated as determined by blood tests (complete blood count [CBC], Chem panel, weight data; Hainfeld et al 2018, Unpublished Results), the long-term persistence of the inert AuNPs in liver and spleen and skin
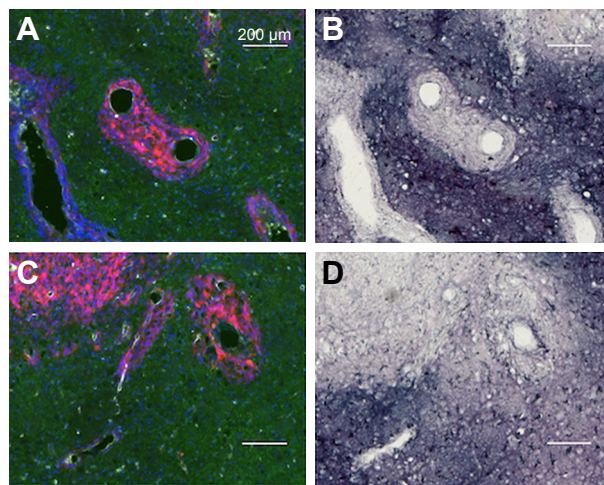
Figure 7 Directly injected AuNPs are largely found in the edema surrounding the tumor cells in peritumor region but not in and around the tumor cells themselves.
Notes: (**A** and **C**) Left hemisphere and (**B** and **D**) left hemisphere, gold enhanced. (**A–C**) mCherry red (tumor, red), anti-albumin (edema, green), DAPI (nuclei, blue), and anti-CD31 (blood vessels, white) and (**B** and **D**) gold enhanced (gold stained, black).
Abbreviations: AuNPs, gold nanoparticles; CD31, cluster of differentiation 31.

Figure 8 Quantification of the percentage of F98 containing BVs (F98 [+] BV) that also contained either a relatively large amount of AuNPs (AuNP++) or a relatively smaller amount of AuNPs (AuNP+) in the main tumor mass or in the peritumor region after either the direct infusion of AuNPs into the tumors or IV injection of AuNPs.
Abbreviations: AuNPs, gold nanoparticles; BV, blood vessel; IV, intravenous.

discoloration issues might be drawbacks to their clinical use. For this reason, we have explored the possibility of directly depositing the AuNP into the region of the brain tumor in place of IV injection. Previously, it was shown by Bobyk et al[24] that the instillation of 250 µg AuNP (AuroVist) directly into the F98 glioma space by CED followed by a single 15 Gy radiation dose resulted in an 8-day extension of median survival compared to rats that received radiation only.

In this article, a histological examination of the distribution of AuNPs in the brains of rats after either IV injection or CED has been performed. After IV injection, AuNPs localized specifically to the region of the main tumor mass (Figure 2). This result is similar to that seen with the dye Evans Blue that also localizes to the tumor region due to the leakiness of the vessels in the tumor.[9] However, whereas Evans Blue has a molecular weight of 961 Da but binds to albumin (68 kDa) and AuroVist (15 nm) is roughly equivalent to a 150 kDa protein molecule, they appear to leak through the compromised BBB (ie, blood tumor barrier [BTB]) similarly. Figure 2E and F particularly reveals that the tumor evinces a rim of heightened edema (rim of brighter green) and remarkably the AuNPs extend to the edge of this edematous band. Thus, passive leak, enhanced permeability and retention (EPR)[23] is seen to be a very effective mode of AuNP delivery to an F98 brain tumor and to the tumor edema. Tumor cells found around BVs proximal and distal to the main tumor mass (Figure 4) appear to be coated with AuNPs forming a cobblestone-like appearance that could be examined further
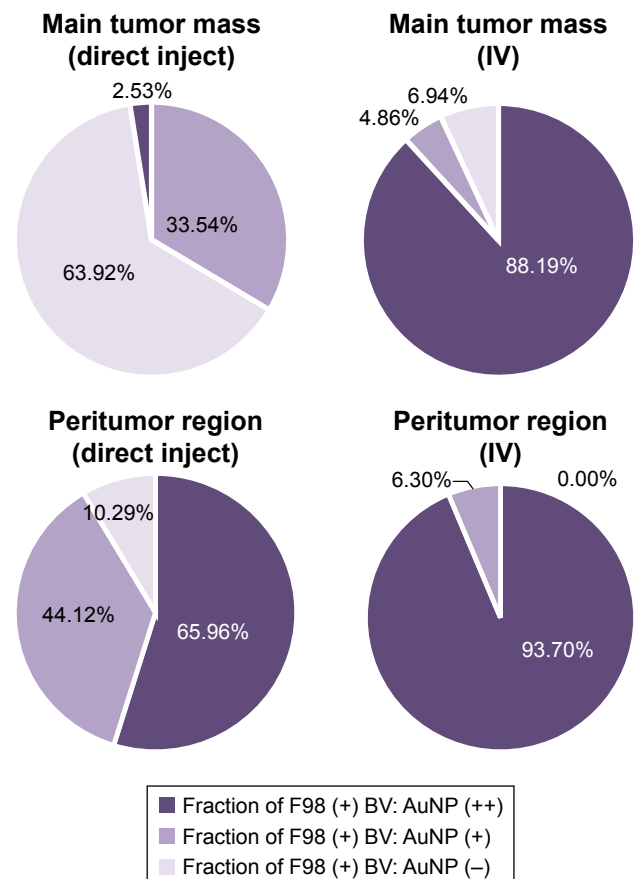
by electron microscopy. Gold lining of tumor cells was not seen in saline-injected controls (Figure 4C and D) indicating that the visually-enhanced AuNPS surrounding tumor cells are the result of IV AuNP injection. Recent theoretical calculations suggest that gold particles coating the surface of tumor cells could effectively increase the radiation dose to tumor cells, particularly in cases where the tumor cell nucleus is close to the cell membrane.[25]

Figure 6 shows the distribution of AuNPs in the brain after direct instillation of 2 mg AuNPs in 10 µL by CED. A large arc of gold can be seen along the external capsule and corpus callosum – white matter tracts along which high-grade glioma cells also migrate. Some of the gold, also in the region of the main tumor mass, is concentrated into cell-like structures that have been identified as microglia and astrocytes (Figure 9). These intensely stained cell-like structures also exist in the white matter tracts. Interestingly, the tumor cells themselves appear to have less gold staining than the surrounding region of brain (Figures 6 and 7). It is possible that the extracellular
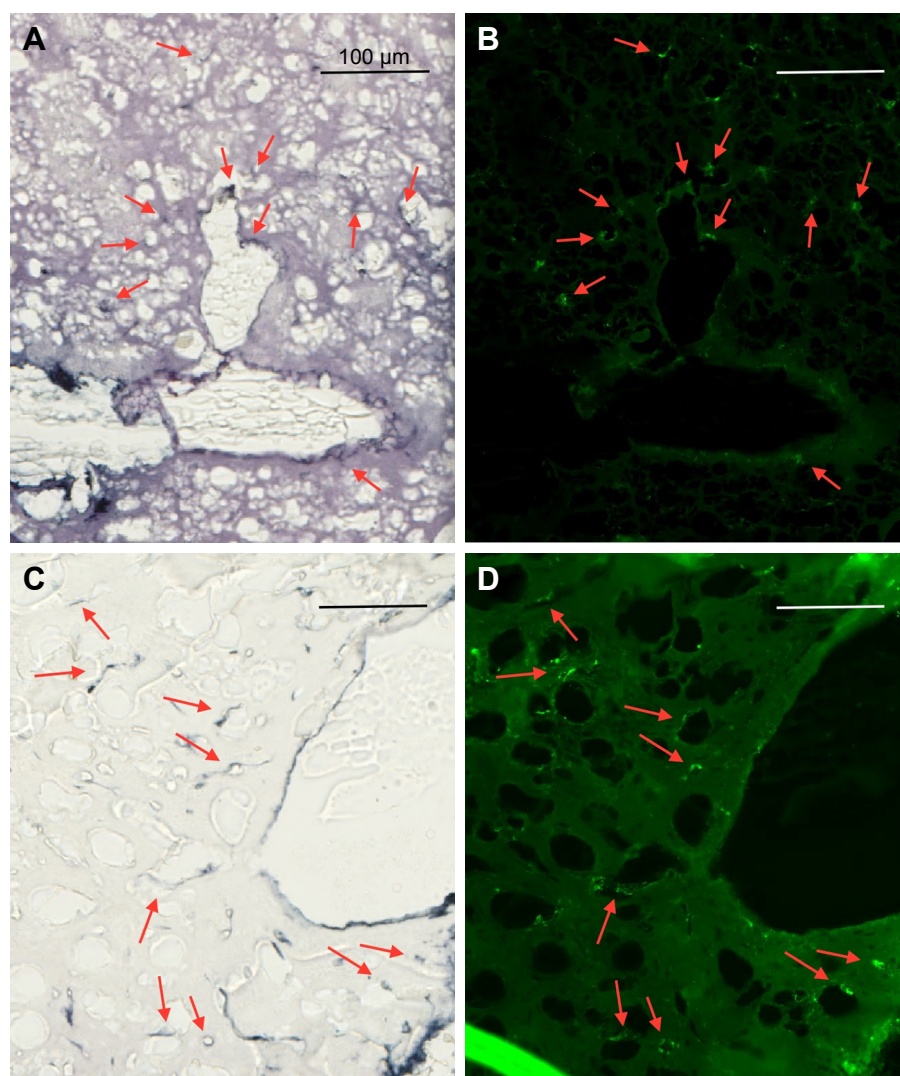
Figure 9 Uptake of AuNPs into brain microglia and astrocytes after injection of AuNPs directly into control brains (non-tumor).
Notes: (**A** and **C**) Gold enhanced (gold stained, black); (**B**) fluorescence, anti-Iba-1 (microglia, green); and (**D**) fluorescence, anti-GFAP (astrocytes, green).
Abbreviations: AuNPs, gold nanoparticles; GFAP, glial fibrillary acidic protein.

matrix of the tumor[26] prevents the access of AuNPs to the tumor cells when the AuNPs are introduced directly into the brain. Tumor malignancy grade is correlated with an increase in diffusion barriers for small molecules,[27] and there is evidence to suggest that collagen may act as a physical barrier to the diffusion of nanoparticles into solid tumors.[28]

Recently, it has been stated that nanoparticles will not gain access to human tumors via the EPR effect since human tumors grow more slowly than rodent tumors and that the EPR effect is not valid in humans.[29] Much literature, however, supports a role for the EPR effect in many human tumors including gliomas. A human trial using radioactive liposomes showed exquisite tumor localization and uptake via the EPR effect.[30] Human gliomas are notoriously leaky and produce large amounts of edema, and numerous publications map brain tumors in relation to their edematous surrounding.[4,30–35]

In fact, human brain tumors are diagnosed on the basis of gadolinium compounds leaking out of tumor BVs through the compromised BBB using MRI.

Our data have shown that after IV injection, AuNPs not only reach the majority of tumor cells in the central tumor mass but also access the peritumor edema, the growing tumor edge, and most of the glioma cells that have migrated far from the central tumor mass. Some migrating tumor cells may not be associated with AuNPs – but most are. This is consistent with the conclusions drawn from other studies not using AuNPs – that migrating tumor cells traveling along BVs alter the permeability from the tight blood–brain barrier to one that passes larger molecules. One study found that "encasing of vessels by gliomas disrupts astrocyte–vascular coupling" and "importantly, single glioma cells are sufficient to locally open the BBB".[9] That would mean that even a single migrating glioma

cell could be accessed with dose-enhancing nanoparticles. Why then are IV-injected chemotherapeutic drugs not very effective for humans' brain tumors as well as the F98 model? Recently, Liu et al[36] showed that systemic BCNU + O^6-benzylguanine only increased F98 median survival by 6 days but, when delivered in nanoparticles, increased median survival to 17 days. When nanoparticles were modified to contain integrin-binding RGD (Arginyl-Lysyl-Aspartic) motif (iRGD), median survival increased to 40 days. The notion that drugs and nanoparticles are poorly effective for brain tumors due to the intact blood–brain barrier (BBB) is prevalent in the literature, eg, Bhowmik et al[37] for BBB review. However, our data suggest that other factors besides an intact BBB need to be invoked to explain the ineffectiveness of systemically delivered drugs, especially for tumors showing extensive disruption of the BBB, such as GBM. For example, drugs typically have a short blood half-life limiting delivery. Nanoparticle constructs may have longer blood half-lives, but they may have other pharmacokinetic problems such as poor release of drug to an active form in the tumor. Other non-BBB factors that impede delivery include brain-to-blood efflux systems, enzymatic activity, plasma protein binding, poor blood flow, and the diffusion blocking tumor microenvironment.[38] It would seem that overcoming the BBB would serve to increase problems with therapeutic specificity, as leakage would occur all over the brain. Attempts to make drugs more lipophilic for better BBB penetration often have reduced effectiveness due to their higher uptake in peripheral tissues thus lowering blood concentration.[38] Our data suggest that the manifold efforts to increase the access of therapeutics through the BTB would seem to be especially helpful for the development of brain tumor therapies.

What are the implications for radiation therapy? We have already shown that IV-injected AuNPs significantly enhance radiation therapy of advanced gliomas using the Tu2449 glioma model.[8] Because of the significantly different gold distributions between IV and CED administration, a comparison of the efficacy of heavy atom-enhanced radiation therapy should be investigated. Since directly instilled AuNPs are concentrated into microglia and astrocytes, one might expect radiation toxicity as microglia and astrocytes would receive large radiation doses. Furthermore, the direct instillation of AuNPs into the brain tumor might be very different from the instillation of AuNPs into the brain after the surgical removal of the tumor. Hence, the potential therapeutic value of directly instilled AuNPs requires further investigation possibly using more therapeutically relevant model systems in which the AuNPs are deposited into the brain after the surgical removal of the tumor, for example. In addition, gadolinium nanoparticles (GdNPs) directly injected into U87 gliomas growing subcutaneously on the legs of mice have been shown to distribute heterogeneously, which might be expected to decrease their overall efficacy.[39]

Significance and conclusion

The data show that IV-injected AuNP delivery is more specific and reaches migrating tumor cells better than direct infusion into the tumor region. IV-injected AuNPs may thus have a greater therapeutic benefit than the direct infusion of AuNPs suggesting a novel strategy for brain tumor radiation therapy that largely overcomes the main problems faced by radiation oncologists. Currently, it is not possible to irradiate both the main tumor mass and the large portions of brain that contain renegade tumor cells with curative radiation doses. Such irradiations would be too toxic to normal brain structures. However, if enough heavy atom nanoparticles can be loaded into tumor cells that are both in the main tumor mass and throughout the brain surrounding the BVs lined with migrating tumor cells, it might be possible to irradiate larger regions of the brain with lower radiation doses. Tumor cells throughout the brain that have accumulated AuNPs will have their radiation doses augmented. The greater the accumulation of heavy atom nanoparticles into and around the tumor cells, the greater the efficacy of metal-enhanced radiation therapy will be. The study presented here suggests that IV administration of heavy atom nanoparticles could be highly effective in treating gliomas and possibly other cancers, especially as new methods are devised to further increase nanoparticle delivery to tumors.[40,41]

Acknowledgments

Disclosure

References

1. Lu J, Cowperthwaite MC, Burnett MG, Shpak M. Molecular predictors of long-term survival in glioblastoma multiforme patients. *PLoS One*. 2016;11(4):e0154313.
2. Scherer H. A critical review: the pathology of cerebral gliomas. *J Neurol Psych*. 1940;3(2):147–177.
3. Hartmann M, Jansen O, Egelhof T, Forsting M, Albert F, Sartor K. Einfluß des Hirnödems auf das Rezidivwachstum maligner Gliome. *Radiologe*. 1998;38(11):948–953.
4. Watanabe M, Tanaka R, Takeda N. Magnetic resonance imaging and histopathology of cerebral gliomas. *Neuroradiology*. 1992;34(6):463–469.
5. Hainfeld JF, Slatkin DN, Smilowitz HM. The use of gold nanoparticles to enhance radiotherapy in mice. *Phys Med Biol*. 2004;49(18):N309–N315.

6. Hainfeld JF, Dilmanian FA, Slatkin DN, Smilowitz HM. Radiotherapy enhancement with gold nanoparticles. *J Pharm Pharmacol*. 2008;60(8): 977–985.

7. Hainfeld JF, Dilmanian FA, Zhong Z, Slatkin DN, Kalef-Ezra JA, Smilowitz HM. Gold nanoparticles enhance the radiation therapy of a murine squamous cell carcinoma. *Phys Med Biol*. 2010;55(11): 3045–3059.

8. Hainfeld JF, Smilowitz HM, O'Connor MJ, Dilmanian FA, Slatkin DN. Gold nanoparticle imaging and radiotherapy of brain tumors in mice. *Nanomedicine*. 2013;8(10):1601–1609.

9. Watkins S, Robel S, Kimbrough IF, Robert SM, Ellis-Davies G, Sontheimer H. Disruption of astrocyte–vascular coupling and the blood–brain barrier by invading glioma cells. *Nat Comm*. 2014;5:1–15.

10. Cuddapah VA, Robel S, Watkins S, Sontheimer H. A neurocentric perspective on glioma invasion. *Nat Rev Neurosci*. 2014;15(7):455–465.

11. Cho SH. Estimation of tumour dose enhancement due to gold nanoparticles during typical radiation treatments: a preliminary Monte Carlo study. *Phys Med Biol*. 2005;50(15):N163–N173.

12. Lechtman E, Chattopadhyay N, Cai Z, Mashouf S, Reilly R, Pignol J. Implications on clinical scenario of gold nanoparticle radiosensitization in regards to photon energy, nanoparticle size, concentration and location. *Phys Med Biol*. 2011;56(15):4631–4647.

13. Kobayashi N, Allen N, Clendenon NR, Ko L-W. An improved rat brain-tumor model. *J Neurosurg*. 1980;53(6):808–815.

14. Allard E, Passirani C, Benoit J-P. Convection-enhanced delivery of nanocarriers for the treatment of brain tumors. *Biomaterials*. 2009; 30(12):2302–2318.

15. Debinski W, Tatter SB. Convection-enhanced delivery to achieve widespread distribution of viral vectors: predicting clinical implementation. *Curr Opin Mol Ther*. 2010;12(6):647–653.

16. Munson JM, Shieh AC. Interstitial fluid flow in cancer: implications for disease progression and treatment. *Cancer Manag Res*. 2014;19(6): 317–328.

17. Pietra G, Johns L. Confocal- and electron-microscopic localization of FITC-albumin in H2O2-induced pulmonary edema. *J Appl Physiol*. 1996;80(1):182–190.

18. Barth RF. Rat brain tumor models in experimental neuro-oncology: the 9L, C6, T9, F98, RG2 (D74), RT-2 and CNS-1 gliomas. *J Neurooncol*. 1998;36(1):91–102.

19. Yamamoto M, Ueno Y, Hayashi S, Fukushima T. The role of proteolysis in tumor invasiveness in glioblastoma and metastatic brain tumors. *Anticancer Res*. 2002;22(6C):4265–4268.

20. Reardon DA, Freeman G, Wu C, et al. Immunotherapy advances for glioblastoma. *Neuro Oncol*. 2014;16(11):1441–1458.

21. Cheema TA, Wakimoto H, Fecci PE, et al. Multifaceted oncolytic virus therapy for glioblastoma in an immunocompetent cancer stem cell model. *Proc Natl Acad Sci U S A*. 2013;110(29):12006–12011.

22. Jain R. Measurements of tumor vascular leakiness using DCE in brain tumors: clinical applications. *NMR Biomed*. 2013;26(8):1042–1049.

23. Senger DR, Galli SJ, Dvorak AM, Perruzzi CA, Harvey VS, Dvorak HF. Tumor cells secrete a vascular permeability factor that promotes accumulation of ascites fluid. *Science*. 1983;219(4587):983–985.

24. Bobyk L, Edouard M, Deman P, et al. Photoactivation of gold nanoparticles for glioma treatment. *Nanomedicine*. 2013;9(7):1089–1097.

25. Sung W, Ye SJ, McNamara AL, et al. Dependence of gold nanoparticle radiosensitization on cell geometry. *Nanoscale*. 2017;9(18): 5843–5853.

26. Wade A, Robinson AE, Engler JR, Petritsch C, James CD, Phillips JJ. Proteoglycans and their roles in brain cancer. *FEBS J*. 2013; 280(10):2399–2417.

27. Vargová L, Homola A, Zámečník J, Tichý M, Beneš V, Syková E. Diffusion parameters of the extracellular space in human gliomas. *Glia*. 2003;42(1):77–88.

28. Mattix B, Moore T, Uarov O, et al. Effects of polymeric nanoparticle surface properties on interaction with brain tumor environment. *Nano Life*. 2013;3(04):1343003.

29. Danhier F. To exploit the tumor microenvironment: Since the EPR effect fails in the clinic, what is the future of nanomedicine? *J Controlled Release*. 2016;244:108–121.

30. Harrington KJ, Mohammadtaghi S, Uster PS, Glass D, Peters AM, Vile RG, Stewart JS. Effective targeting of solid tumors in patients with locally advanced cancers by radiolabeled pegylated liposomes. *Clin Cancer Res*. 2001;7(2):243–254.

31. Engelhorn T, Savaskan NE, Schwarz MA, et al. Cellular characterization of the peritumoral edema zone in malignant brain tumors. *Cancer Sci*. 2009;100(10):1856–1862.

32. Morita K-i, Matsuzawa H, Fujii Y, Tanaka R, Kwee IL, Nakada T. Diffusion tensor analysis of peritumoral edema using lambda chart analysis indicative of the heterogeneity of the microstructure within edema. *J Neurosurg*. 2005;102(2):336–341.

33. Dubois LG, Campanati L, Righy C, D'Andrea-Meira I. Gliomas and the vascular fragility of the blood brain barrier. *Front Cell Neurosci*. 2014;8:418.

34. Gillespie DL, Flynn JR, Ragel BT, Arce-Larreta M, Kelly DA, Tripp SR, Jensen RL. Silencing of HIF-1α by RNA interference in human glioma cells in vitro and in vivo. *Methods Mol Biol*. 2009;487:283–301.

35. Rieken S, Habermehl D, Mohr A, et al. Targeting α v β 3 and α v β 5 inhibits photon-induced hypermigration of malignant glioma cells. *Radiat Oncol*. 2011;6(1):132.

36. Liu C, Yao S, Li X, Wang F, Jiang Y. iRGD-mediated core-shell nanoparticles loading carmustine and O6-benzylguanine for glioma therapy. *J Drug Targeting*. 2017;25(3):235–246.

37. Bhowmik A, Khan R, Ghosh MK. Blood brain barrier: a challenge for effectual therapy of brain tumors. *BioMed Res Intl*. 2015;2015.

38. Banks WA. Characteristics of compounds that cross the blood-brain barrier. *BMC Neurol*. 2009;9 Suppl1:S3.

39. Carmona A, Roudeau S, L'Homel B, Pouzoulet F, Bonnet-Boissinot S, Prezado Y, Ortega R. Heterogeneous intratumoral distribution of gadolinium nanoparticles within U87 human glioblastoma xenografts unveiled by micro-PIXE imaging. *Analyt Biochem*. 2017;523:50–57.

40. Maeda H, Nakamura H, Fang J. The EPR effect for macromolecular drug delivery to solid tumors: Improvement of tumor uptake, lowering of systemic toxicity, and distinct tumor imaging in vivo. *Adv Drug Deliv Rev*. 2013;65(1):71–79.

41. Wilhelm S, Tavares AJ, Chan WCW. Analysis of nanoparticle delivery to tumours. *Nat Rev Mat*. 2016;1:16014.